CFD modelling of vented explosions for chambers of two different scales

Guillaume Lecocq, Jérôme Daubech, Emmanuel Leprette

CFD modelling of vented explosions for chambers of two different scales

Guillaume Lecocq [a], Jérôme Daubech [a] & Emmanuel Leprette [a]

Institut National de l'Environnement Industriel et des Risques, Parc Technologique ALATA, BP 2, 60550 Verneuil-en-Halatte, France

E-mail: guillaume.lecocq@ineris.fr

Abstract

Numerous practical uses of hydrogen imply a container, this latter containing process equipment and even hydrogen storage devices. Scenarios of confined explosions are often identified during risk analyses of such installations and related overpressure effects should be quantified.

CFD is theoretically attractive for vessels equipped with one or more vents as geometrical effects are intrinsically accounted for. Nevertheless, the physical sub-models of the CFD approach that are used to quantify flame speeds may vary from a modelling to another as well as the physical explanation of flame acceleration.

In this paper, CFD computations inspired of recent works (Tolias, 2018) are carried out for comparison with numerous measurements of explosions in a 4 m^3 chamber, free of obstacle, containing a homogenous H_2/air mixture (Duclos, 2019). Different mixture compositions are considered as well as several initial turbulent intensities. This step enables a first assessment of the CFD model.

Another set of computations is performed for a 37 m^3 chamber, also free of obstacle, with multiple vents in order to study the robustness of the model predictions when changing the flammable cloud length scale as well as the venting method. The limits of the modelling are finally discussed.

Keywords: *vented explosion, scale effect, hydrogen, CFD*

1. Introduction

Hydrogen is more and more used in the industrial processes in order to contribute to their decarbonization. In practice, hydrogen-based processes are often packaged in sea containers.

A representative but simplified configuration could be an electrolyser installed inside a container, surrounded with numerous pipes for conveying water and the separated gases, eventually large capacity storage vessels and a power supply network, all these elements occupying about at least 30 % of the container inner volume. Doors enable to access the technical zones of the container.

A risk analysis dedicated to this equipment could identify a scenario of a large flammable volume formation inside the container in case of hydrogen leak in the process. If an ignition occurs, a flame will be generated and propagate inside the container with a pressure rise leading to doors or vents opening, if these latter are present. At this stage, if the fresh gases are not totally burned, they can be ejected outside the container where a secondary explosion occurs due to flame propagation in the ejected flammable volume.

The pressure effects of such explosion have to be quantified for the safety study related to the equipment. Computational Fluid Dynamics (CFD) is an attractive tool for addressing an explosion in a container as numerous geometrical effects are at stake. Accounting for them could theoretically bring more accuracy in the results when compared to another approach involving approximations in

the problem description. Nevertheless, performing a CFD modelling is not straightforward as it requires skills in numerical methods, knowledge of the explosion physics and of the capacities of the physical sub-models (turbulence, flame / turbulence interaction, …). Numerous CFD approaches were provided in the literature for modelling vented explosions for empty boxes, notably by Bauwens (2011), Molkov (2012) and Tolias (2018). Roughly, they are built in a similar manner but with different sub-models, which is notably explained by the different points of view of the authors concerning numerical models, explosion physics and modelling.

The current paper aims at contributing to the reflexion around the CFD modelling of vented explosion, this one being limited to free of obstacle enclosures. To meet this objective, two configurations are considered:

- A 4 m^3 enclosure with a 0.7 m x 0.7 m vent in which homogenous hydrogen/air mixtures can be ignited. The mixture can be turbulent before ignition or quiescent. Three hydrogen volume fractions are considered.
- A 37 m^3 vessel on which are mounted several vents, the total surface being conserved. The dimensions of this vessel are close to those of a 20 ft ISO container. A single equivalence ratio is studied.

CFD computations are performed for each geometry with an approach similar to the one published by Tolias in order to 1) assess if the choice of a set of sub-models can be used for modelling vented explosions with variations of the initial turbulence, hydrogen volume fraction and geometry and 2) evaluate whether the physics of the external explosion can be identified with such modelling or not.

2. Experimental set-ups

Numerous explosion tests were carried out by Duclos (2019) with an enclosure whose length, width and height are respectively 2 m, 2 m and 1 m. Homogenous flammable H_2/air mixtures were generated in the box. The parameters of interest were the initial hydrogen volume fraction and the initial turbulence intensity. The mixture is ignited at the centre of a 2 m x 1 m face and the 0.7 m x 0.7 m vent is located on the opposite face. Figure 1 shows the location of the pressure sensors.

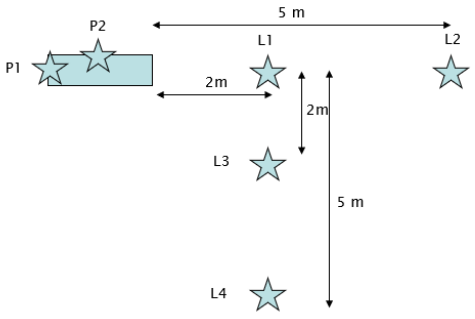

Fig. 1. *Locations of the pressure sensors for the 4 m^3 enclosure. View from the top.*

Tests that will be studied in the paper are listed in the Table below. Note the turbulence was experimentally characterized with a turbulent length scale and a fluctuating velocity.

Table 1: *Retained parameters values for modeling the 4m³ vented explosions. Bold values correspond to adjustments of the original values supplied by Molkov (2012)*

Test	**Hydrogen volume fraction**	**Regime before ignition**	**Damköhler number (in initial conditions)**	**Karlovitz number (in initial conditions)**
4 and 36	16 %	Laminar	Undefined	Undefined
24 and 25	16 %	Turbulent ($u' = 2{,}3$ m/s, $L_t = 3{,}2$ cm)	20	30
-	21 %	Laminar	Undefined	Undefined
23	21 %	Turbulent ($u' = 5$ m/s, $L_t = 7$ cm)	35	70
26	25 %	Laminar	Undefined	Undefined
28	25 %	Turbulent ($u' = 4{,}5$ m/s, $L_t = 7$ cm)	70	60

Daubech et al. (2022) supply results of another experimental campaign with explosions in a larger scale enclosure. It is indeed 2.5 m wide and high and 6 m long. H_2 / air homogenous mixtures were formed in the box and the one considered in the current paper, with a hydrogen volume fraction of 15.5 %, was ignited on the small face. The mixture was quiescent before ignition. Venting was ensured by four 0.3 m x 0.4 m vents with an opening pressure of 50 mbar. Two configurations are regarded for the opening surface distribution: either they are grouped on the face opposite to the ignition location or they are split on two faces of the enclosure (Figure 2). The location of the pressure sensors can be seen in Figure 3.

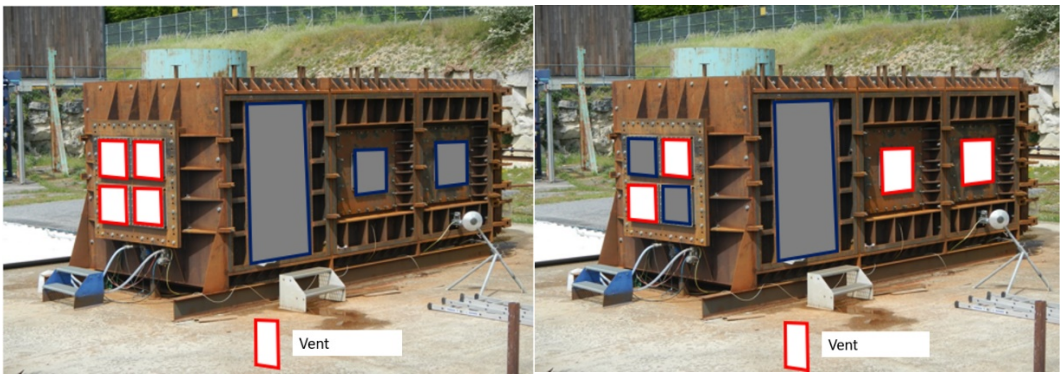

Fig. 2. *View of the 37 m³ enclosure and of the possible locations of the vents (in red). Left: configuration 1, right: configuration 2. Panels in blue are safety vents which should not open during the explosion.*

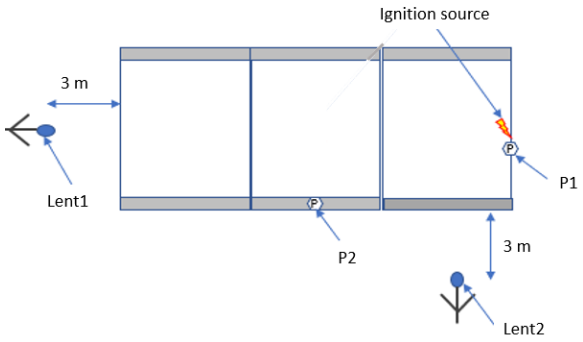

Fig. 3. *Location of the ignition source and pressure sensors for the 37 m³ confined explosions (P1, P2: inside pressure – Lent1, Lent2: outside pressure*

3. Phenomenology related to vented explosions and CFD modelling

3.1 Phenomenology

If the mixture is initially quiescent, after the ignition phase the flame front is expected to self-accelerate due to Darrieus-Landau and thermo-diffusive instabilities as it was previously observed for spherical lean hydrogen flames (Bauwens, 2017). If there is an initial turbulence, the flame front acceleration is due to both intrinsic flame instabilities and flame / turbulence interaction. According to lab-scale tests, the flame front wrinkling for a given wave number can be dominantly by one phenomenon or the other depending both on the ratio of the fluctuating velocity, u', and the laminar flame speed S_L and on the Karlovitz number (Yang, 2018).

When moving, the flame pushes the fresh gases that flow out of the enclosure once a vent is open. Depending on the propagation history of the flame inside the enclosure, the outer flow of fresh gases might differ when the flame exits the enclosure. Roughly, if the flame comes out of the box shortly after fresh gases ejection, the flame will propagate in a vortex, if it exits the enclosure later, propagation will occur in a jet. According to a numerical study, in the first case, turbulence is localized to the shear layer surrounding the jet that pushes the vortex (Daubech, 2016). In the second case, it is possible to encounter on a more extended area a more intense turbulence. According to Tolias (2018), it seems that the external explosion effects can be explained mostly by a flame / turbulence interaction. Other authors like Bauwens (2011) and Keenan (2014) estimate the Rayleigh-Taylor instability, related to a sudden acceleration of the flame front when it exits the enclosure, plays a significant role in the pressure effects generation in the external explosion.

3.2 Available approaches in the literature

CFD approaches available in the literature for vented explosions mostly rely on Large Eddy Simulation (LES) for turbulence modeling. Nevertheless, applying this method is very expensive in terms of computational resources as the non-resolved kinetic energy should remain below 20 % (Pope, 2004). A RANS framework is then preferred in the current paper.

Among the available models for CFD modeling of vented explosions, the one of Tolias et al. (2018) relies on a RANS framework.

Tolias et al. approach is based on the k-ϵ model including the modification of Kato-Launder for turbulent correlation closures.

The chemical source term which pilots the propagation speed of the flame front is simply closed as the product of the gradient of the progress variable ($\tilde{c}$), the volume mass of the fresh gases (ρ^u) and a characteristic flame speed: $\overline{\rho}\,\widetilde{\dot{\omega}_c} = \rho^u S_F |\nabla \tilde{c}|$. The flame speed $S_F$then writes: $\Xi.S_L$ where Ξ is a wrinkling factor. As evocated previously, the lean hydrogen flames are prone to thermo-diffusive

instabilities. The choice of closure for the chemical source term implicitly assumes that differential diffusion effects, responsible of these instabilities, are not accounted for by the diffusion operator in the transport equations. Furthermore, a proper modelling of instabilities might need a sufficient resolution of the flame front thickness by the mesh, which is not encountered in RANS modeling.

The wrinkling factor Ξ has to account for all physical phenomena that locally impact the flame speed. In the work of Tolias et al., the wrinkling factor is decomposed in a product of wrinkling factors representing independently the effect of a single phenomenon (turbulence, instabilities, flame-generated turbulence) on the flame front velocity: $\Xi = \Xi_t \Xi_k \Xi_{lp}$. Most of CFD approaches that deal with under-resolved modeling of explosions rely on a similar approach (Molkov, 2012 and Bauwens, 2011). Recently, Lapenna et al. (2021) proposed a similar sub-grid scale modeling from DNS studies of small-scale premixed flames.

Ξ_t models the flame / turbulence interaction. It is closed with the model of Schmid et al. (1998) that can be applied in all turbulent combustion regimes. $\Xi_t = 1 + u'/S_L(1 + Da^{-2})^{-1/4}$ where Da is the Damköhler number. Ξ_k accounts for the effect of flame-generated turbulence, a phenomenon drive by hydrodynamic instability and Ξ_{lp} enables to integrate the effect of differential diffusion on the flame speed. Both models were originally proposed by Molkov (2012). They integrate a progressive increase of the corresponding wrinkling factor with the flame radius (R) towards a maximum value. Thus, $\Xi_k = 1 + (\psi \Xi_{k,max} - 1)(1 - \exp(R/R_{0k}))$ with $\Xi_{k,max} = (\tau - 1)/\sqrt{3}$, τ being the thermal expansion rate and $\Xi_{lp} = \Xi_{lp}^{max}/2(1 + \tanh((R - R_{0lp})/0.01))$. Molkov (2012) proposed values for the remaining parameters that depend on the hydrogen volume fraction of the hydrogen / air mixture. According to their formulation, the models for Ξ_k and Ξ_{lp} seem to be designed for flames with an hemispherical or spherical shape.

3.2 Approaches retained

The computations presented in the current work are based on a modelling strategy close to the one of Tolias. The transport equations are solved for momentum, pressure, a progress variable and energy with a pressure-based solver of the CFD code OpenFoam (Weller, 1998). Nevertheless, turbulence is modelled with a standard k- ϵ model and while the chemical source term closure of Tolias et al. was kept, the reference radius R_{0k} appearing in the expressions of Ξ_k was adjusted to the computed configurations in order to get a predicted pressure peak inside the enclosure at the same time as the measured one. Furthermore, for a volume fraction of 16 %, the value of Ξ_k^{max} was increased of 50 %, in order to recover the internal peak pressure. Table 2 shows the parameters values retained.

Table 2: *Retained parameters values for modeling the 4m³ vented explosions. Bold values correspond to adjustments of the original values supplied by Molkov (2012)*

Hydrogen volume fraction	S_L **(m/s)**	τ **(-)**	R_{0lp} **(m)**	Ξ_{lp}^{max} **(-)**	Ξ_k^{max} **(-)**	R_{0k} **(m)**	ψ **(-)**	**Reduction factors for turbulent cases**
16 %	0.505	4.5	0.01	2	**3**	**0.5**	1	0.5
21 %	0.9	5.75		2	(τ -1)/ $\sqrt{3}$=2,75	**0.2**	1	0.27
25 %	1.5	6.45		1,7	(τ -1)/ $\sqrt{3}$=3,15	**0.8**	**0.8**	0.37

For the explosion in the 4m³ chamber, the computational domain was 22 m long, 20 m wide and 11 m high. It was composed of 5 million hexahedra with a cell size of 4 cm on the flame path. The mesh for the largest chamber, covering a 14 m x 20 m x 12 m domain was made of 5 million hexahedra, the smallest being 4 cm wide.

4. Case of the 4 m^3 chamber

Figure 3 highlights, for an initially quiescent mixture with a hydrogen volume fraction of 16 %, the pressure signals measured inside the enclosure at two locations, P1 and P2, and outside the box on the axis of the vent. It appears that signals P1 and P2 are distinct whereas identical signals could be expected inside the enclosure for all tests carried out on this enclosure. The reason for this specificity is not known to date. All CFD computations predict same signals for P1 and P2.

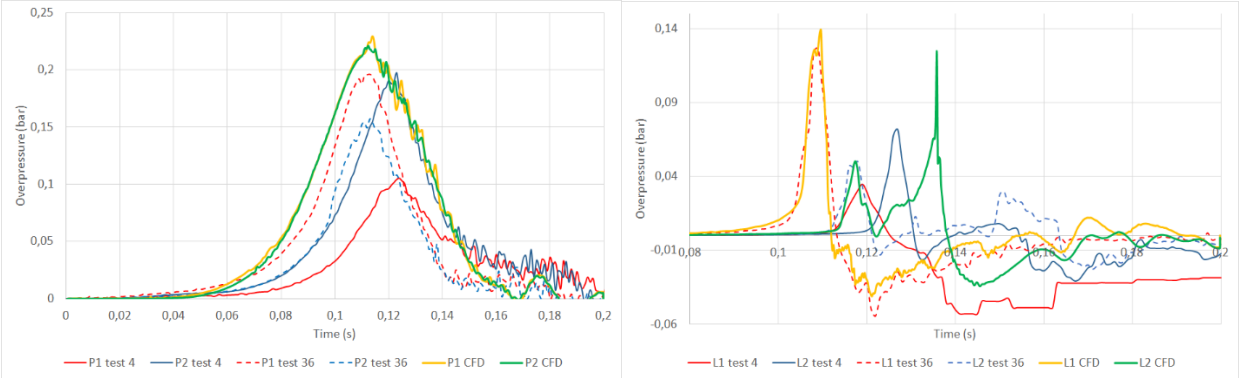

Fig. 3. Case of the initially quiescent mixture with a hydrogen volume fraction of 16 %. Comparison of the computed and measured pressure signals inside (left) ou outside (right) the 4 m^3 enclosure.

While initial conditions are similar, the signals obtained for the two tests 4 and 36 are different but both give an envelope of what should be predicted. CFD slightly overestimates the P2 peak of the test 36 but accurately recovers the L1 pressure signal. The first part of the L2 signal is predicted but unphysical secondary peak appears at 0.12 s. This secondary peak is related to a sudden flame acceleration on the jet axis due to very large values reached (about a few hundreds) by the parameter Ξ_t when the flame reaches the tip of the flammable cloud.

It can be noted here that modelling an experiment with numerous pressure probes is more challenging but brings a safer assessment basis: the L2 signal shows the qualitative agreement of the predicted explosion with the measured one is not fully representative.

Comparison of numerical prediction and measurements for a hydrogen volume fraction of 21 % (Figure 4) shows a P2 pressure peak approached and a large overestimation (about 100 %) for pressure peak L1. The time agreement for pressure peak occurrence inside the box for measurement and prediction seems to lead to a time agreement for the pressure peak occurrence outside of the enclosure.

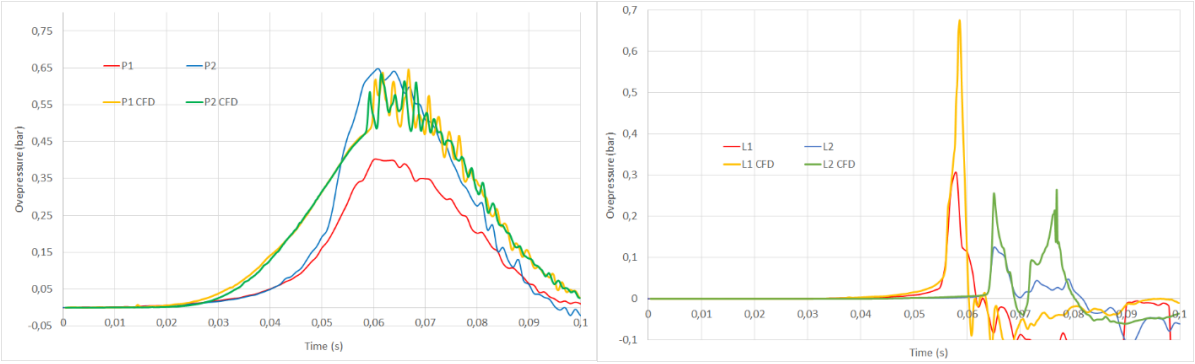

Fig. 4. Case of the initially quiescent mixture with a hydrogen volume fraction of 21 %. Comparison of the computed and measured pressure signals inside ou outside the 4 m^3 enclosure.

The observations made for the 21 % hydrogen volume fraction case can be kept for the 25 % hydrogen volume fraction case (Figure 5).

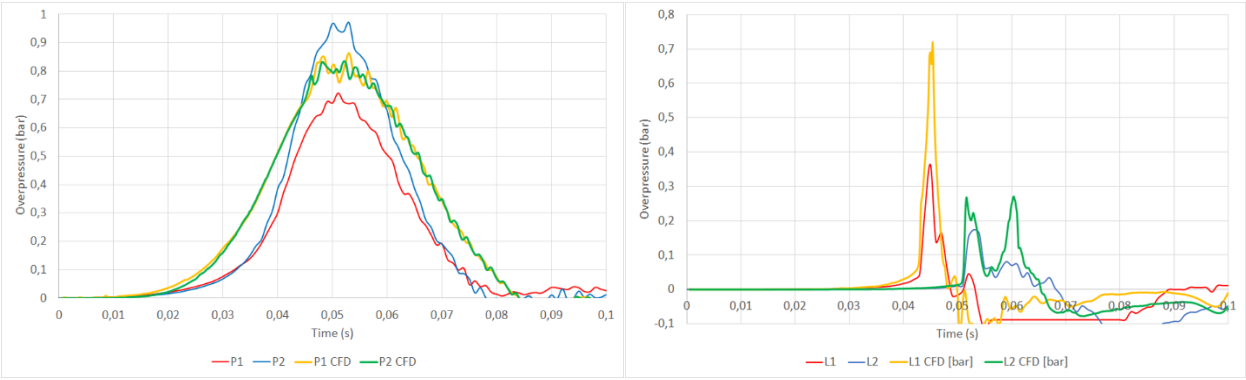

Fig. 5. Case of the initially quiescent mixture with a hydrogen volume fraction of 25 %. Comparison of the computed and measured pressure signals inside ou outside the 4 m^3 enclosure.

Finally, a case for which the velocity field inside the enclosure is turbulent before ignition is considered. For this one the hydrogen volume fraction is 21 % and turbulence is characterized by a fluctuating speed of 5 m/s and an integral length scale of 7 cm. With a Karlovitz number of 70, the combustion regime is, according to the combustion diagram (Peters, 2000), a thickened-wrinkled reaction sheet. The model that was used for the quiescent case is kept, the impact of initial turbulence being accounted for in the initialization of the scalar $\tilde{k}$ and $\tilde{\epsilon}$. This modelling (not shown) led to significant overestimation of all pressure peaks. It was chosen to multiply the chemical source term with a damping factor in order to retrieve the pressure signal inside the enclosure. A value of 0.27 has to be taken. It can be seen as a correction for the prediction of instabilities effects when turbulence exists before ignition.

Introducing this correction factor, the pressure signal P2 is recovered (Figure 6), but the pressure peak outside of the box close to the vent, measured in L1, is overestimated (about 100 %).

For other turbulent cases with hydrogen volume fraction of 16 % or 25 %, in the same way a damping coefficient lower than 0.5 should be applied to the chemical source term to recover the pressure signal in P2 (Table 2).

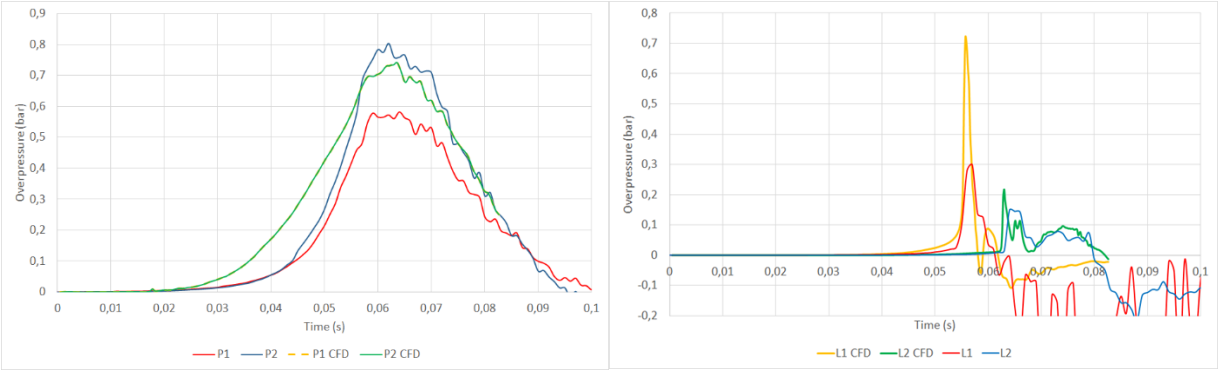

Fig. 6. Case of the initially turbulent mixture with a hydrogen volume fraction of 21 %. Comparison of the computed and measured pressure signals inside (left) and outside (right) the 4 m^3 enclosure.

It appears that the model inspired by Tolias et al. with the set of parameters given by Molkov for the sub-models accounting for the instability effects may require adaptations, at least in the case of the 4 m^3 enclosure for recovering inner pressure signal. This could be explained by the shape of the box in which the flame is elongated and not spherical.

If the mixture is initially turbulent, the chemical source term has to be damped by a coefficient which ranges from 0.3 to 0.5, depending on the hydrogen volume fraction. This shows a limit to the generic character of the model which should be applied only for initially quiescent mixtures.

The predicted pressure peak in L1 is either equal or well higher than the measured one. It is possible that the $k-\epsilon$ model produces too much turbulence outside the enclosure and/or the assumption of an equilibrium turbulent speed reached instantaneously during flame / turbulence interaction is too conservative.

A secondary peak is predicted for the L2 signal. This one is not existing in reality or is largely overestimated. It is explained by a sudden acceleration on the flame axis when approaching the tip of the flammable cloud. The causes of this can be similar the ones mentioned above for L1 signal.

5. Case of the 37 m^3 chamber

The CFD model is, in this section, applied to the case of the explosion of a quiescent and homogenous hydrogen / air mixture with a hydrogen volume fraction of 15.5 % in the 37 m^3 chamber. In the computation, the progressive opening of the vent was not modelled. Each vent was replaced with a permanent opening.

The CFD modelling proposed for a 16 % flammable volume in the 4 m^3 chamber was retained. The computation led to an overestimation of the inner pressure peak. In order to retrieve the final pressure peak, the parameter Ξ_k^{max} was divided by 2.

Figure 7 compares the measured and computed inner pressure signals for configuration 1 and 2. The effect of the vent at the beginning of the signal is not retrieved., nevertheless, in both cases the order of magnitude of the pressure peak is recovered.

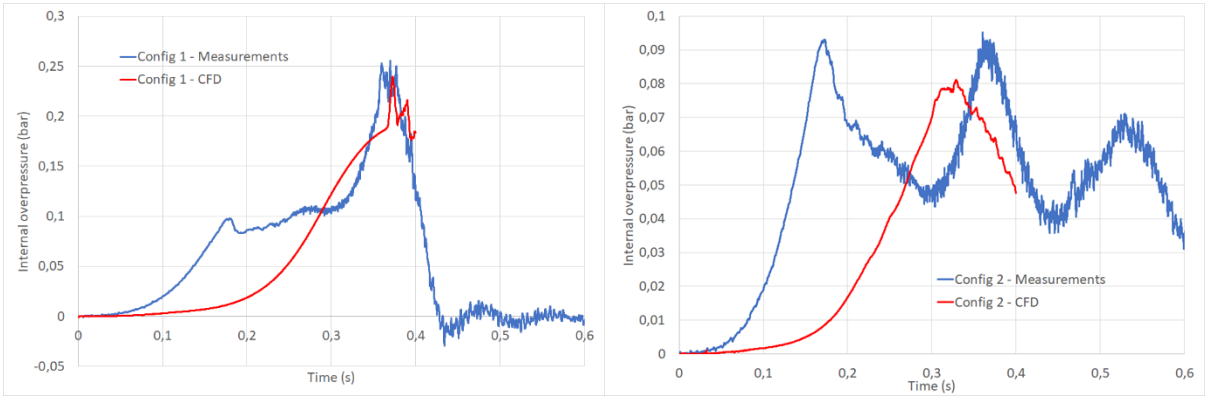

Fig. 7. Comparison of the measured and computed pressure signals inside the 37 m^3 enclosure for the two configurations.

The external pressure signals outside the chamber can be seen in Figure 8 and 9 for configurations 1 and 2. For configuration 1, the measured pressure peak at L1 is about 50 mbar while the CFD model predicts a peak of 280 mbar. For configuration 2, the measured peak is 25 mbar and the predicted one is 20 mbar.

At the pressure probe L2, the maximum measured pressure is 25 mbar for configuration 1 and 7 mbar for configuration 2 and the respective predicted values are 20 and 14 mbar. The orders of magnitude are recovered.

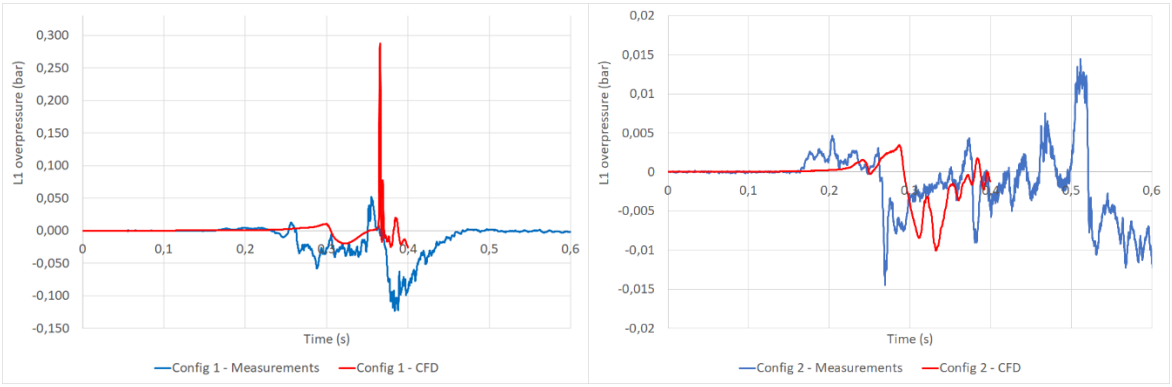

Fig. 8. Comparison of the measured and computed pressure signals at the pressure probe L1 outside the 37 m^3 enclosure for the two configurations.

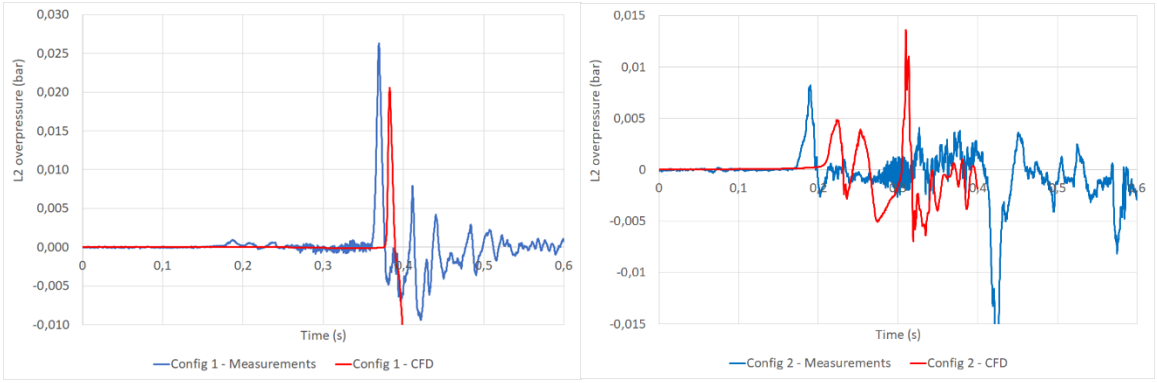

Fig. 9. Comparison of the measured (left) and computed (right) pressure signals at the pressure probe L2 outside the 37 m^3 enclosure for the two configurations.

Once more, it appears that the modeling of instabilities in the CFD model is not generic and that the model used should also depend to the geometry. The section of the combustion chamber is a square whereas it was rectangular in the smallest chamber. This may explain that Ξ_k^{max} had to be adjusted.

The global sequence of the explosion related to configuration 1 first appears similar to the explosion in the small combustion chamber. Nevertheless, the outer flammable cloud is different when the flame exits the enclosure. The outer flammable cloud appears as a jet while in the case of the 4 m^3 chamber took the shape of a large vortex. The overestimation of the prediction of the pressure peak in L1 can be explained by an exaggerated production of turbulence by the $k-\epsilon$ model, by an equilibrium assumption for the flame speed and maybe by missing a physical feature. Local extinction phenomena could be encountered.

6. Conclusions

Computations were performed for vented explosions with varying parameters (hydrogen volume fraction, initial turbulence and geometry). They aimed at verifying if a CFD model similar to these encountered in the literature could predict all these cases.

It appeared that the model for the effects of instabilities in the enclosure had to be modified for certain hydrogen volume fraction and geometries for recovering inner pressure peaks. If initial turbulence was present in the enclosure, a damping factor has to be introduced whose value is difficult to quantify a priori.

The peak pressure of most of the external explosions was overpredicted. It can be due to an overestimation of the turbulence production outside of the box, the assumption of a turbulent flame speed reaching instantaneously its equilibrium value or a part of physics which is missing, like maybe local extinction.

Going deeper in that work is needed to propose a generic way to model the effects of the instabilities on the flame inside the enclosure.

Concerning the external explosion, the pressure effects can be explained by a flame / turbulence interaction. Nevertheless, the outer fresh gases flow should be studied in detail in order to identify the reason the CFD approach of the paper overestimates the pressure effects of the external explosion.

Acknowledgements

This work was granted access to the HPC resources of TGCC under the allocation 2021-A0102B11482 made by GENCI (Grand Equipement National de Calcul Intensif)

References

I.C. Tolias et al. (2018) An improved CFD model for vented deflagration simulations – Analysis of a medium-scale hydrogen experiment. *International Journal of Hydrogen Energy* 43(52), pp. 23568-23584

A. Duclos (2019) *Développement de modèles phénoménologiques et de maitrise des risques d'explosion pour la filière émergente hydrogène-énergie*. Thesis manuscript. Compiègne Technology University

C.R. Bauwens, J. Chaffee & S.B. Dorofeev (2011). Vented explosion overpressure from combustion of hydrogen and hydrocarbon mixtures. *Int. Journal of Hydrogen Energy*, 36(3): 2329-2336.

Molkov, V. (2012). *Fundamentals of Hydrogen Safety Engineering, parts I & II.* Free download e-book, bookboon.com, ISBN: 978-87-403-0279-0.

J. Daubech, E. Leprette & C. Proust (2022) *Influence of vent distribution on the violence of a gas explosion.* Submitted to ISHMPIE.

C.R. Bauwens et al. (2017) *Experimental investigation of spherical-flame acceleration in lean hydrogen-air mixtures.* International Journal of Hydrogen Energy 42, pp. 7691-7697

S. Yang et al. (2018) *Role of Darrieus-Landau instability in propagation in expanding turbulent flames.* J. Fluid Mech 850, pp. 784-802

J. Daubech, C. Proust, G. Lecocq (2016) *Propagation of a confined explosion to an external cloud*. 11th ISHPMIE

J.J. Keenan, D.V. Makarov & V.V. Molkov (2014) *Rayleigh-Taylor instability: Modelling and effect on coherent deflagrations*. International Journal of Hydrogen Energy 39, pp. 20467-20473.

S.B. Pope (2004) *Ten questions regarding the large-eddy simulation of turbulent flows*. New journal of Physics 6.

H.-P. Schmid et al. (1998) *A model for calculating heat release in premixed turbulent flames*. Combust. Flame 113, pp. 79-91

Lapenna et al. (2021) *Subgrid modeling of intrinsic instabilities in premixed flame propagation*. Proc. Combust. Inst. 38(2), pp. 2001-2011

Weller, H.G, Tabor, G. (1998). A tensorial approach to computational continuum mechanics using object-oriented techniques. *Computational Physics*, 12: 620-631.

N. Peters (2000) Turbulent combustion. Cambridge university press.